



## Full length article

## Effect of cell thickness on the electrical and optical properties of thin film silicon solar cell

A.A. Zaki<sup>a,b,\*</sup>, A.A. El-Amin<sup>a,c</sup><sup>a</sup> Physics Department, Faculty of Science, Taibah University, Yanbu, Saudi Arabia<sup>b</sup> Physics Department, Faculty of Science, Benha University, Egypt<sup>c</sup> Faculty of Science, Aswan University, Aswan, Egypt

## ARTICLE INFO

## Article history:

Received 21 February 2017

Received in revised form 31 May 2017

Accepted 9 June 2017

Available online 29 June 2017

## Keywords:

Thin film Si semiconductor different thickness

Electrical properties

Optical properties

## ABSTRACT

In this work Electrical and optical properties of silicon thin films with different thickness were measured. The thickness of the Si films varied from 100 to 800  $\mu\text{m}$ . The optical properties of the cell were studied at different thickness. A maximum achievable current density (MACD) generated by a planar solar cell, was measured for different values of the cell thickness which was performed by using photovoltaic (PV) optics method. It was found that reducing the values of the cell thickness improves the open-circuit voltage ( $V_{oc}$ ) and the fill factor (FF) of the solar cell. The optical properties were measured for thin film Si (TF-Si) at different thickness by using the double beam UV-vis-NIR spectrophotometer in the wavelength range of 300–2000 nm. Some of optical parameters such as refractive index with dispersion relation, the dispersion energy, the oscillator energy, optical band gap energy were calculated by using the spectra for the TF-Si with different thickness.

© 2017 Elsevier Ltd. All rights reserved.

## 1. Introduction

Many work has been reported in the field of semiconductors because they are applied scientifically and technologically [1]. They are used in solid state devices and infrared optical fibers, that depend on optical constants [2,3]. Silicon (Si) is one of the fundamental parts in many electronic devices especially for integrated circuits and solar cells. The thin film Si Photovoltaic technique is used for the base of display industries [4]. Because silicon is an indirect band gap material, the reciprocal of absorption coefficient for sunlight must be less than the thickness of Si [5–9]. The effects of temperature during film growth and post-deposition thermal annealing on the optical and electrical properties for thin-film silicon solar cell were investigated [10,11]. The electrical and optical properties of Si-doped indium tin oxides as transparent electrodes and anti-reflection coatings for Si-based solar cells were studied [12].

In order to obtain a sufficient absorption of sunlight, the film thickness of Si must be more than 700  $\mu\text{m}$  which is considered a large thickness and is not preferable for commercial production

of the solar cells because of its high cost and its low effect for the collection of photogenerated carriers [13–17]. Adjusting the multireflections and surface characteristics of the cell enhance the absorption of a thinner film. Spectrophotometry is considered a good method for measuring the optical properties of the Si thin film used. The optical constants of p- and n-type silicon samples, having plane-parallel faces, with a UV-Vis-NIR spectrophotometer at room temperature were measured. The Wemple–DiDomenico dispersion model for real refractive index of silicon slabs was used [18]. Spectroscopic and UV-visible spectrophotometry technique were used to determine the energy gap and optical properties of Ge thin films of various thicknesses synthesized with electron beam evaporation technique [19]. The refractive index and optical energy gap of a multilayer sample were studied via spectroscopic ellipsometry [20]. The refractive index dispersion from the transmission spectrum of a semiconductor thin film was calculate [21]. Many optical parameters such as index of refraction, extinction coefficient and band energy that could be calculated from the transmission and absorption of light are essential for variable applications [22].

The change in the thickness of silicon solar cell has a strong influence on their performance and efficiency. In this work Si solar cells of different thickness were prepared and studied carefully for measuring their electrical and optical constants as a function of thickness.

\* Corresponding author at: Physics Department, Faculty of Science, Benha University, Egypt.

E-mail addresses: [ayman\\_a73@hotmail.com](mailto:ayman_a73@hotmail.com) (A.A. Zaki), [aelamin2000@yahoo.com](mailto:aelamin2000@yahoo.com) (A.A. El-Amin).

## 2. Experimental work

The processing techniques and structure for the manufacturing and design of a thin solar cell are important for solving many problems such as the low cost substrate and the endure of high temperatures for Si film. The deposition process of Si, the metallization technique and formation of PN junction must be suitable for different thickness varying from 100  $\mu\text{m}$  to 800  $\mu\text{m}$ . Moreover, the grain size, the active-layer quality, the interface texture nature and the high reflectivity of the back contact were taken into account in the cell design. It was known that, as the grain size increases, the device performance becomes better. Also, the interface recombination influences the cell parameters [23,24].

The film of  $\mu\text{c-Si}$  based solar cell contains a two-layer structure of a p-type and an n-type region, one of which is much thicker than the other (Fig. 1). The typically p-type which is the cell base region, was deposited on a substrate of glass coated with Al metal. The deposition process occurred at low-temperature using chemical vapor deposition (CVD) and hot-wires CVD techniques. Since the decreasing in the cell thickness leads to an increase in the metallic loss, an adjustment was made between the metallic loss and the minimum thickness of the cell. In addition to maintaining the integrity of the substrate and rear metal layer, a low-temperature process can minimize the diffusion of dopant along grain boundaries by the high-efficiency design. An electric field is formed over the p-n junction. Photocarriers are mainly generated in the field free region in the thick lightly doped layer. The thickness of the cell film was determined by using a thickness mentor ASTM D6132 of accuracy  $\pm 1 \mu\text{m}$  equal which 2% of reading and minimum individual layer thickness from 50 microns to 2 mm [25–29].

All silicon thin films used in this study were deposited by (CVD). The CVD process took place at a total gas flow of 40 sccm and gas pressure of 2 Pa, the substrate temperature ( $T_s$ ) of 120  $^\circ\text{C}$ , filament temperature ( $T_f$ ) of 1500  $^\circ\text{C}$ . The thicknesses of n-layer were 100–800  $\mu\text{m}$  and that of p-layer was 1000  $\mu\text{m}$ . The models of solar cell with structures of Al/n-Si/pSi/Al were prepared. The deposition conditions and properties of n-type films were measured using thickness mentor.

The thermal Evaporation (CVD) technique involves heating a solid material inside a high vacuum chamber, till some vapor pressure is produced. The evaporated material condensed on surfaces in the chamber is coated as a thin film. This is one of the best methods for controlling the thickness of the cell by using quartz crystals. This type of measurement and control shows that an oscillator crystal is placed inside the vacuum chamber to receive deposition in an actual time. The oscillation frequency will decrease as the crystal's mass increases by the material being deposited on it. After that an electronic instrument continuously reads the frequency and performs appropriate mathematical functions to convert that frequency data to thickness data.

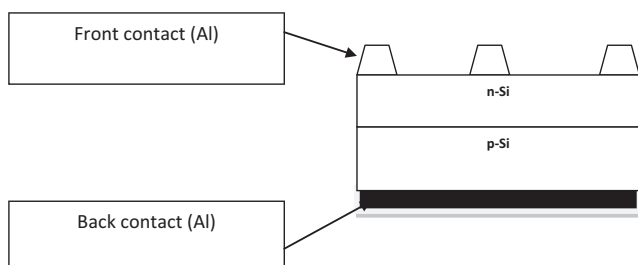


Fig. 1. A structure of the prepared solar cell.

UV–Visible spectrum gives information about the structure of the molecules that causes electronic excitation from lower to higher energy state. The optical transmission spectra of the TF-Si were recorded using a double beam UV–Vis–NIR spectrophotometer (UV-1800 SHIMADZU, Japan) with a wavelength ranging from 300 to 2000 nm at normal incidence of light at 27  $^\circ\text{C}$ .

## 3. Results and discussion

Obviously, reducing the thickness of the cell reduces absorption and thus reducing the photocurrent of it. Fig. 1, shows the relation between current density, and basic voltage where the short circuit current density ( $I_{sc}$ ), and open circuit voltage ( $V_{oc}$ ) parameters of the cell were measured during dark conditions.

The photocurrent shown in Fig. 2 was the optimal achievable current density for the AM1.5 solar spectrum. The current increases with increasing the film thickness up to 700  $\mu\text{m}$  but decreases again with decreasing the resistance. At the thickness 800  $\mu\text{m}$  the photocurrent decreases because the absorption increases, this clarifies that the thickness 700  $\mu\text{m}$  was the best value for obtaining high-efficiency solar cell.

Fig. 3 shows the relation between open-circuit voltage ( $V_{oc}$ ) and the thickness of the cell. Increasing the film thickness leads to decreasing the  $V_{oc}$  till 700  $\mu\text{m}$  and then the  $V_{oc}$  tend to increase again. Although reducing the thickness of the cell leads to an increase in the  $V_{oc}$ , the excess of the carrier recombination at the surface of the cell causes an opposite effect.

In Fig. 4 the spectra for tested solar cells were measured with different thickness of Si films (100, 200, 300, 400, 500, 600, 700 and 800  $\mu\text{m}$ ). Also, when the thickness of the cell increases the value of maximum  $I_{sc}$  increases and shifts towards the red and infra red reign. Until 700  $\mu\text{m}$  thickness, the efficiency of the cell increases due to the higher spectral sensitivity of Si in the red region than in the blue one, and then the maximum  $I_{sc}$  decreases at the thickness of 800  $\mu\text{m}$ .

### 3.1. Refractive index dispersion

The transmittance of different Si thin films were measured at wavelengths ranging from 350 to 2000 nm as illustrated in Fig. 5. This figure shows that, each thickness of Si envelops of maxima  $T_{max}$  and minima  $T_{min}$  of transmission shows interference pattern in the visible and near infra red region. The inverse relation between the transmittance and the thickness of Si thin films at certain wavelength was verified in Fig. 6. Also, Fig. 7 shows the direct

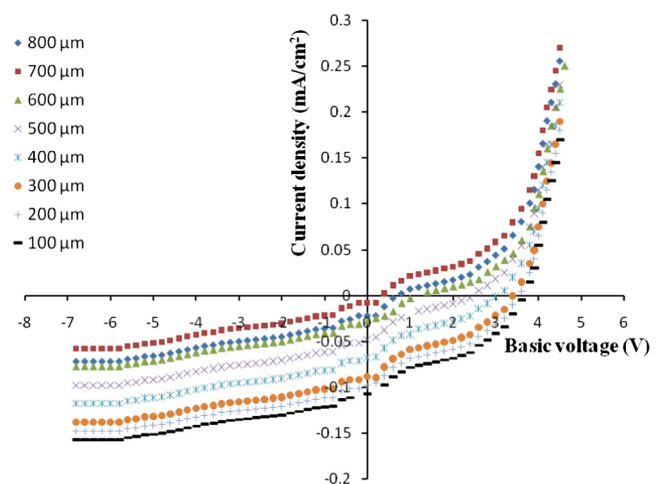
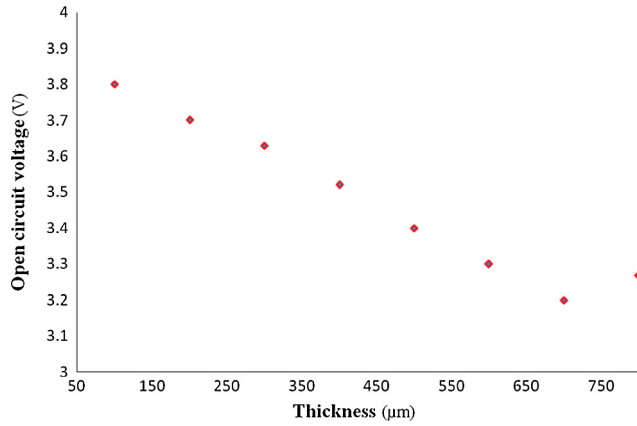
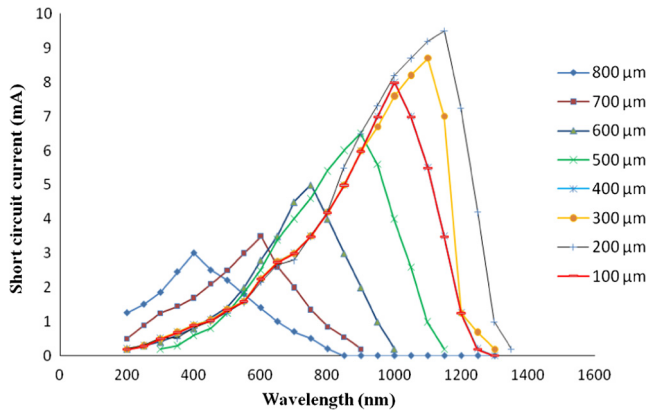


Fig. 2. Current – voltage characteristic in dark at different thickness.



**Fig. 3.**  $V_{OC}$  of a Si solar cell as a function of thickness for high and low surface recombination velocities.



**Fig. 4.** Spectral response for different cell thickness of TF-Si.

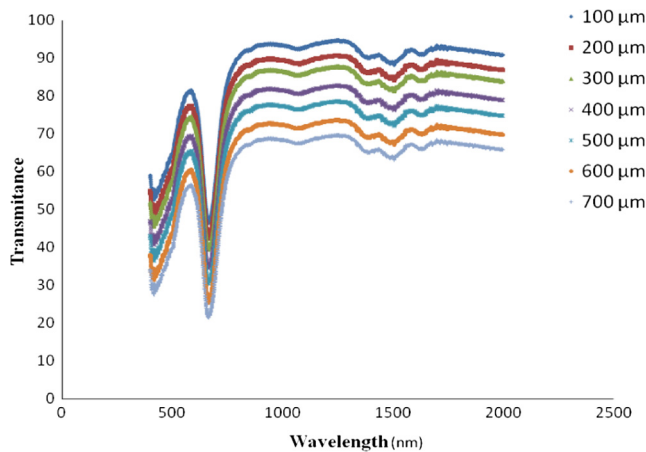


**Fig. 5.** The optical transmission spectra for different thickness of TF-Si.

reflectance relation with the thickness of Si thin films at wavelengths ranging from 400 to 1500 nm.

The index of refraction of each film was determined from the transmission spectra at maxima and minima values by using the envelope methods of Swanepoel expression [30]:

$$n = \sqrt{N + (N^2 - n_s^2)^{1/2}} \quad (1)$$

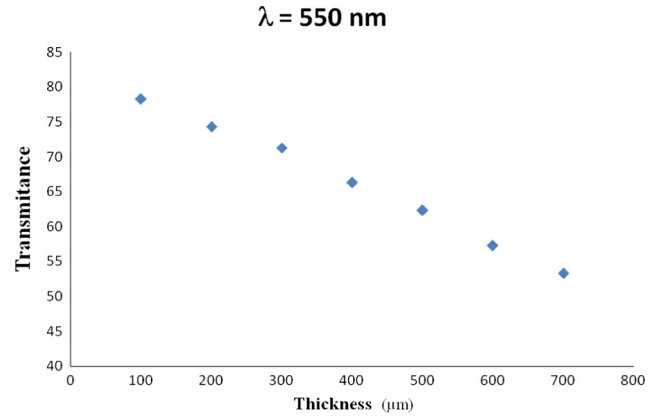


**Fig. 6.** The relation between the transmittance and the thickness of Si thin films at 550 nm wavelength.

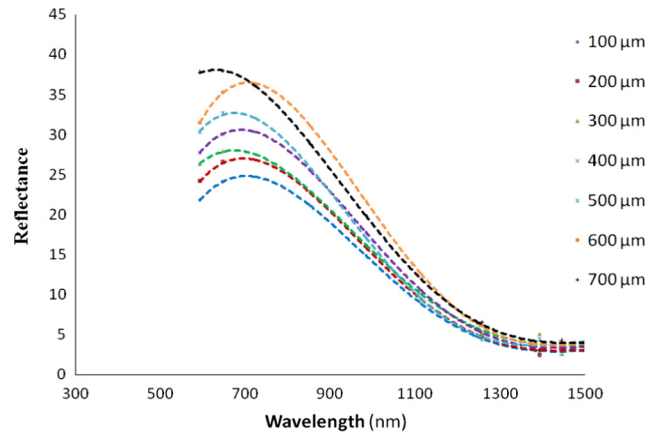


**Fig. 7.** The reflectance relation for different thickness of Si thin films with wavelengths.

where

$$N = 2n_s \left( \frac{T_{max} - T_{min}}{T_{max} + T_{min}} \right) + \frac{n_s^2 + 1}{2}$$

where  $n_s$  is the index of refraction of the substrate used, which is nearly constant for wavelengths larger than 350 nm and equal 1.43 in this work and was calculated from the transmittance of a glass substrate ( $T_s$ ) by using the relation [31]:

$$n_s = \frac{1}{T_s} + \sqrt{\frac{1}{T_s^2} - 1} \quad (2)$$

It is clear from Fig. 8 that the index of refraction of Si thin film decreases with increasing the wavelength. Also the refractive index of the Si thin film increases with increasing the thickness because the excess of layers may reduce the porous structure i.e., an increase in the closeness and compactness of the film molecules. The values of refractive indices are plotted together with the best fit in Fig. 8 where the dots are the values calculated from the transmission spectrum and the solid lines represent the curve fitting by using Cauchy dispersion relationship, which can be used to extrapolate the dependence of wavelength beyond the range of measurements [32]:

$$n(\lambda) = A + \frac{B}{\lambda^2} \quad (3)$$

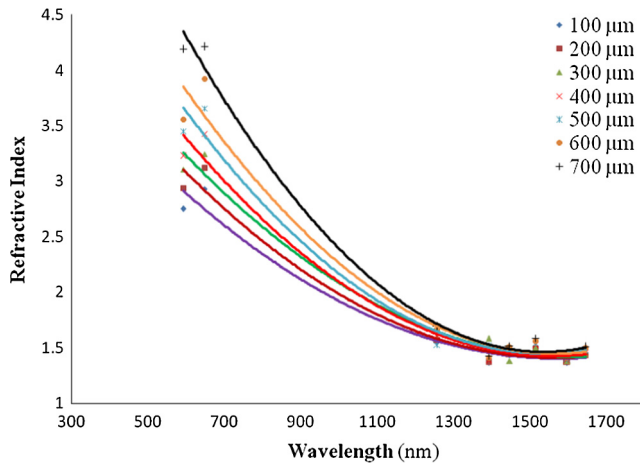


Fig. 8. The dispersion of refractive index and wavelengths at different thickness of Si films.

The least square fitting of the Cauchy's parameters A and B for different thickness of Si film are listed in Table 1.

The refractive index dispersion  $n$  was calculated also from the single-effective-oscillator model by using Wemple and Di Domenico [33,34].

$$n^2 = 1 + \frac{E_d E_o}{E_o^2 - (h\nu)^2} \quad (4)$$

$$(n^2 - 1)^{-1} = \frac{E_o}{E_d} - \frac{(h\nu)^2}{E_d E_o} \quad (5)$$

where  $E_d$  is the strength of oscillator or dispersion energy and  $E_o$  is the oscillator energy which is the energy separated between conduction and valence bands. By plotting  $(n^2 - 1)^{-1}$  with  $(h\nu)^2$  and fitting a linear function the values of  $E_o$  and  $E_d$  was obtained from the slope and the intercept as in Fig. 9 by using Eq. (5). The values of  $E_o$  and  $E_d$  for all thickness of thin film samples were measured in Table 1.

### 3.2. The absorption coefficient, optical band gap and extinction coefficient

The optical absorption coefficient  $\alpha$  can be obtained from the envelope around the maxima [35–37] by:

$$\alpha = -\frac{1}{d} \ln \frac{E_M - [E_M^2 - (n^2 - 2)^3 (n^2 - n_s^2)]^{\frac{1}{2}}}{(n^2 - 1)^3 (n - n_s^2)} \quad (6)$$

where

$$E_M = \frac{8n^2 n_s}{T_M} + (n^2 - 1)(n^2 - n_s^2)$$

where  $d$  is the thickness of Si film and  $T_M$  is the maximum transmission. Moreover the extinction coefficient,  $k$  was given by:

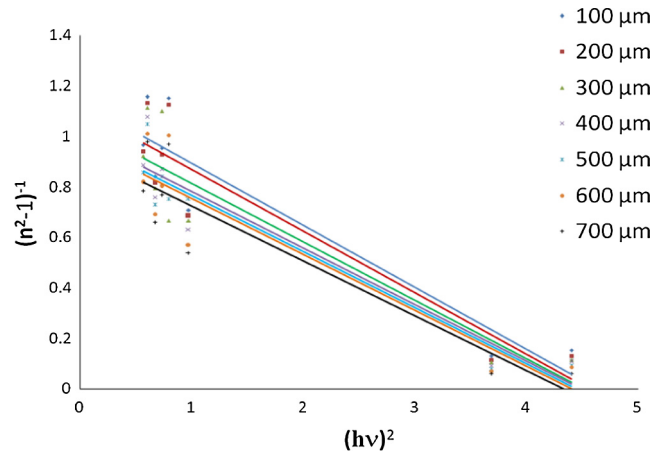


Fig. 9. the refractive index  $(n^2 - 1)^{-1}$  versus  $(h\nu)^2$  for different thickness of Si thin films.

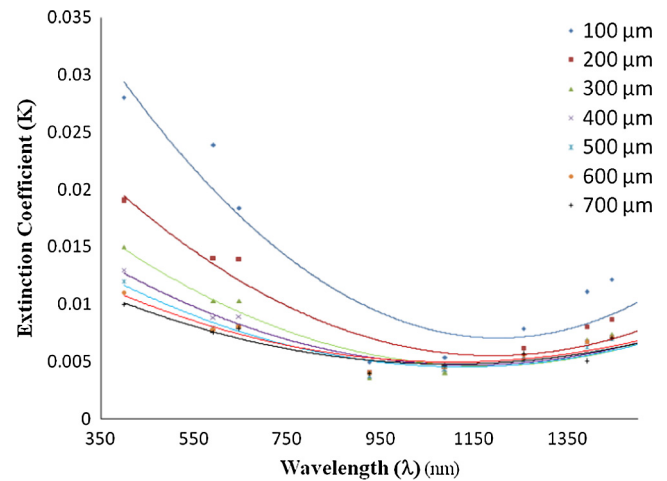


Fig. 10. Dispersion of extinction coefficient,  $k$  with wavelength for Si films at different thickness.

$$k = \frac{\alpha \lambda}{4\pi} \quad (7)$$

Fig. 10 shows the extinction coefficient  $k$  with wavelength for variable thickness of Si thin films. It was noted that  $k$  exhibits decrease with increasing film thickness and wavelength and then it increases slightly again. Obviously, the decrease is due to the absorption band and the increment again maybe due to high reflectance. Furthermore, with difference in thickness, the absorption and extinction coefficients change a little bit.

The energy gap  $E_g$  and allowed optical transitions in a semiconductor film Si were determined by knowing the absorption coefficient as a function of the photon energy using Tauc's law [38–40]:

Table 1

The least square fitting parameters A and B, dispersion energy  $E_d$ , the oscillator energy  $E_o$ , and the energy band gaps  $E_g$  for Si films at variable thickness.

Si film thickness ( $\mu\text{m}$ )	A	B ( $\mu\text{m}$ ) <sup>2</sup>	$E_d$ [eV]	$E_o$ [eV]	Energy gap ( $E_g$ ) (eV)
100	1.1471	0.6358	1.89302	2.156149	2.3
200	1.1206	0.7162	1.923732	2.139189	2.25
300	1.12455	0.7716	2.040731	2.130524	2.2
400	1.0883	0.8398	2.113395	2.121849	2.15
500	1.0639	0.9341	2.133074	2.111743	2.1
600	1.0475	1.0093	2.154277	2.10042	2.08
700	0.9629	1.2201	2.214146	2.081297	2.04



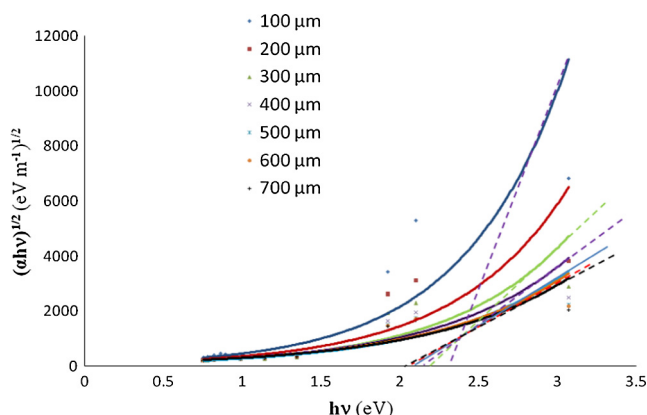


Fig. 11. The plot of  $(\alpha hv)^{1/2}$  versus photon energy ( $h\nu$ ) for Si at different thickness from 100 to 700  $\mu\text{m}$ .

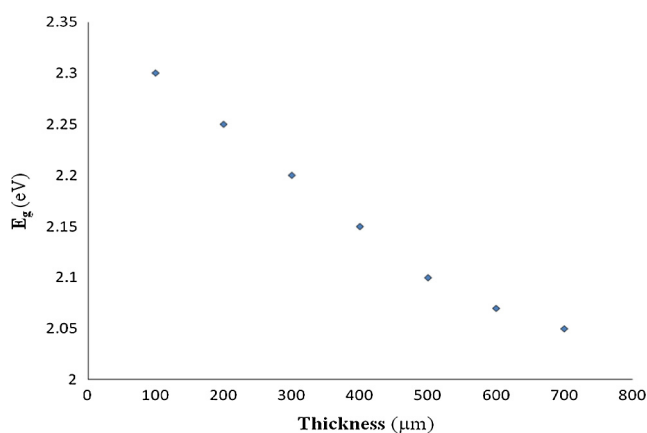


Fig. 12. The plot of energy gap ( $E_g$ ) versus thickness of TF-Si.

$$\alpha hv = B(h\nu - E_g)^m \quad (8)$$

where  $\alpha$  is the absorption coefficient,  $h$  is the Planck's constant,  $\nu$  is the frequency of the incident light  $B$  is a constant and  $m$  is a number which have the values of 1/2, 3/2, 2 and 3, according to the electronic transition.

Since silicon is an indirect band gap material, it was found that the best fit was obtained when  $m$  equals 2, which represents the process of allowed indirect transition. From Eq. (8), by plotting the relation between  $(\alpha hv)^{1/2}$  and photon energy ( $h\nu$ ), the energy band gap  $E_g$  was obtained by the extrapolation of the straight-line portion of this plot to the energy axis ( $h\nu$ ), i.e., at  $\alpha$  equal zero as shown in Fig. 11. Table 1 shows the energy band gaps for Si films of different thickness where the energy gap increases as the film thickness of Si decreases as shown in Fig. 12 [41–44].

#### 4. Conclusion

The electrical and optical properties of Si thin films with thickness (100–700  $\mu\text{m}$ ) were measured. The photocurrent increases with increasing the film thickness up to 700  $\mu\text{m}$  but decreases again at the thickness 800  $\mu\text{m}$  because the resistance decreases and the absorption increases. The thickness 700  $\mu\text{m}$  was the best thickness for obtaining a high-efficiency of the solar cell. The value of maximum  $I_{sc}$  increases and hence the efficiency of the cell increases with increasing the thickness up to 700  $\mu\text{m}$ . The optical parameters of the semiconductor TF-Si at different thickness could be obtained. The optical constants of the Si films of variable thick-

ness (100–700  $\mu\text{m}$ ) were measured by means of transmittance using UV-vis-NIR spectral data at normal incidence of light. The determination of the refractive index as a function of wavelength was calculated by using Cauchy's fitting equation for each thickness of the film. The refractive index–wavelength variation leads to evaluating dispersion and oscillator energies of Si thin films. From the transmittance and absorbance, the absorption coefficient, extinction coefficient and energy band gap were calculated.

#### References

- [1] S. Kumar, M.A.M. Khan, Chalcogenide Lett. 9 (2012) 145–149.
- [2] D.C. Kaseman, I. Hung, Z. Gan, B. Aitken, S. Currie, S. Sen, J. Phys. Chem. B 118 (2014) 2284–2293.
- [3] E.R. Shaaban, I.S. Yahia, M.F. Fadel, J. Alloys Compd. 469 (2009) 427.
- [4] A. Shah, P. Torres, R. Tscharnner, N. Wyrsh, H. Keppner, Photovoltaic technology: the case for thin-film solar cells, Science 285 (1999) 692–698.
- [5] D. Redfield, Appl. Phys. Lett. 25 (1974) 647.
- [6] J. Esher, D. Redfield, Appl. Phys. Lett. 25 (1974) 702.
- [7] K. Gosh, C. Fishman, T. Feng, J. Appl. Phys. 51 (1980) 446–454.
- [8] M. Green, Silicon Solar Cells, University of New South Wales, Sydney, Australia, 1995.
- [9] E. Yablonovitch, G. Cody, IEEE ED-29 (1982) 300.
- [10] J. Park, C. Shin, S. Lee, S. Kim, J. Jung, N. Balaji, V.A. Dao, Y.-J. Lee, J. Yi, Effect of thermal annealing on the optical and electrical properties of boron doped a-SiOx: H for thin-film silicon solar cell applications, Thin Solid Films 587 (2015) 132–136.
- [11] A.A. El-Amin, A.A. Zaki, Improving the Efficiency of multicrystalline silicon by adding an ARC layer in the front device, Silicon 9 (2017) 53–58.
- [12] G. Oh, K.S. Lee, E.K. Kim, Electrical and optical properties of Si-doped indium tin oxides as transparent electrode and anti-reflection coating for solar cells, Curr. Appl. Phys. 15 (2015) 794–798.
- [13] M.A. Green, K. Emery, Y. Hishikawa, W. Warta, "Solar cell efficiency table (version 35), Prog. Photovolt: Res. Appl. 18 (2010) 144.
- [14] K. Taretto, U. Rau, J.H. Werner, Closed-form expression for the current/voltage characteristics of pin solar cells, Appl. Phys. A 77 (2003) 865–871.
- [15] M. S. Anjan, M.Z. Kabir, Modeling of current-voltage characteristics of CdS/CdTe solar cells, in: 4th, International Conference on Optical, Optoelectronic and Photonic Materials and Applications (ICOOPMA 2010), Budapest, Hungary, August 2010.
- [16] K. Yamamoto, A. Nakajima, M. Yoshimi, Toru Sawada, et al., A high efficiency thin film silicon solar cell and module, Sol. Energy 77 (6) (2004) 939–949.
- [17] H. Joshua, J. Huang Carpenter, Chang-Zhi Li, Jun-Sheng Yu, Harald Ade, Highly efficient organic solar cells with improved vertical donor-acceptor compositional gradient via an inverted off-center spinning method, Adv. Mater. 28 (2016) 967–974.
- [18] E.Y. El-Zaiat, G.M. Youssef, Dispersive parameters for complex refractive index of p-and n-type silicon from spectrophotometric measurements in spectral range 200–2500 nm, Opt. Laser Technol. 65 (2015) 106–112.
- [19] E.S.M. Goh, T.P. Chen, C.Q. Sun, Y.C. Liu, Thickness effect on the band gap and optical properties of germanium thin films, J. Appl. Phys. 107 (2010) 024305.
- [20] J. Lopez, E. Solorio, H.A. Borbon-Nunez, Refractive index and bandgap variation in  $\text{Al}_2\text{O}_3$ -ZnO ultrathin multilayers prepared by atomic layer deposition, J. Alloys Compounds 691 (2017) 308–315.
- [21] M.E. Ismail, E.R. Shaaban, M. El-Hagary, A new method for calculating the refractive index of semiconductor thin films retrieved from their transmission spectra, J. Alloy. Compd. 663 (2016) 20–29.
- [22] R.R. Willey, Practical Design and Production of Optical Thin Films, Marcel Dekker Inc., New York, 2002, p. 222.
- [23] R. Bergmann et al., Semicond. Sci. Technol. 12 (1997) 224.
- [24] R. Schropp, M. Zeman, Amorphous and microcrystalline silicon solar cells: modeling.
- [25] B. Sopori, Appl. Opt. 27 (1988) 25.
- [26] H. Craighead, R. Howard, D. Tennant, Appl. Phys. Lett. 37 (1980) 653.
- [27] T. Hansen, C. Johnson, U.S. Patent 4 (1980) 229–233.
- [28] H. Mataré, Defect Electronics in Semiconductors, Wiley-Interscience, New York, 1971.
- [29] D. McLean, Grain Boundaries in Metals, Oxford University Press, New York, 1957.
- [30] R. Swanepoel, Determination of the thickness and optical constants of amorphous silicon, J. Phys. E: Sci. Instrum. 16 (1983) 1214.
- [31] T.S. Moss, Optical Properties of Semiconductors, Butterworth, London, 1959.
- [32] S.H. Wemple, M. Di Domenico, Phys. Rev. B 3 (1971) 1338.
- [33] S.H. Wemple, Phys. Rev. B 7 (1973) 3767.
- [34] J. Tauc, R. Grigorovici, A. Vencu: Phys. Stat Sol. B. Optical properties and electronic structure of amorphous germanium. 15 (1996) 627–637.
- [35] R. Swanepoel, J. Phys. E: Sci. Instrum. 17 (1984) 896.
- [36] J.B. Ramirez-Malo et al., Optical properties of  $\text{As}_2\text{S}_3$  semiconducting glass films of non-uniform thickness deposited by thermal evaporation, Mater. Chem. Phys. 40 (1995) 30–36.
- [37] G.C. Xie et al., Effect of In-doping on the optical constants of ZnO thin films, Phys. Procedia 32 (2012) 651–657.

- [38] J.I. Pankove, *Optical Processes in Semiconductors*, Prentice-Hall, New Jersey, 1971, p. 93.
- [39] J. Tauc, *Amorphous and Liquid Semiconductors*, Plenum, New York, 1974 (Ch. 4).
- [40] E.R. Shaaban, M.M. Soraya, M. Shapaan, H. Shokry Hassan, M.M. Samar, Applying wedge shape model for calculating both film thickness and optical constants of SeSeZn films with high precision for optoelectronic devices, *J. Alloy. Compd.* 693 (2017) 1052–1060.
- [41] S.V. Gaponenko, *Optical Properties of Semiconductor Nanocrystals* Cambridge University Press, Cambridge, 1998.
- [42] A. Shik, *Quantum Wells: Physics and Electronics of Two-Dimensional Systems* World Scientific, Singapore, 1997.
- [43] M. Fox, *Optical Properties of Solids* Oxford University Press, Oxford, 2001. 2.
- [44] A.M. Bakry, Influence of film thickness on optical properties of hydrogenated amorphous silicon thin films, *Egypt. J. Solids* 31 (1) (2008) 11–22.